

Fig. 1. Energy ratios for the levels of even-even nuclides. ● From alpha-particle spectrograph data. × From gamma-ray data.

experimental ratios for 10 nuclei in the heavy element region plotted against neutron number. It is fairly certain that corresponding states are compared here although in only one case, Cm^{242} , have the necessary measurements been made to establish this state as $4+$.⁴ The heaviest nuclei show remarkably close agreement with the expectations for the postulated rotational states and there appears to be a progressive departure from the ratio 3.3 toward lighter nuclei. (There is no convincing justification for plotting these data strictly with respect to neutron number as is done here; in fact, it is not to be expected that the nuclear deformation which defines these levels is simply a function of the neutron number.)

Gamma-ray data have been used to infer the existence of the third *even-spin* state for three species. The ratios of the third to

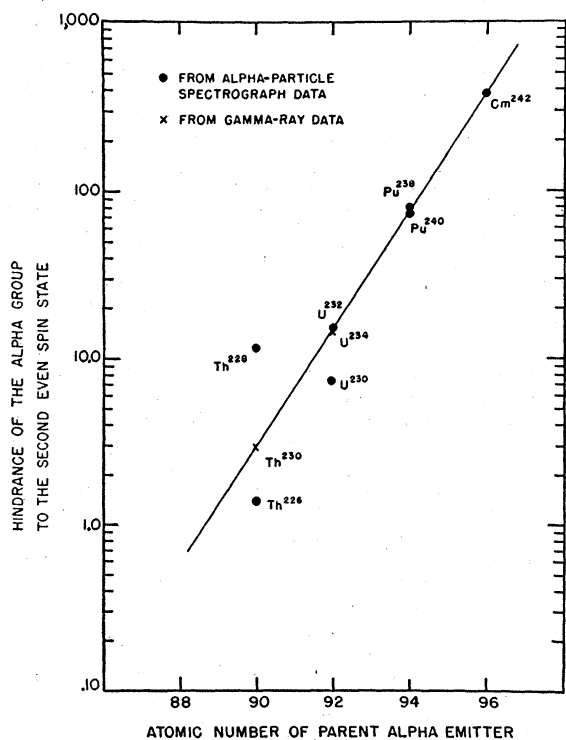


Fig. 2. Relation between the observed partial half-life and that calculated from alpha-decay theory for the alpha group populating the second even-spin state.

the first levels are indicated in Fig. 1 in relation to the theoretical value 7 for the third rotational state, $J=6$.

In the study of the alpha spectra of most of the nuclides shown in Fig. 1, it became clear that the alpha transitions leading to the second even-spin states were highly hindered. That is, the measured partial half-lives were much longer than expected simply from the energy and nuclear charge. (It will be remembered that the ground-state transitions and those leading to the first even-spin states are in first approximation unhindered.) The Cm^{242} alpha group leading to the second even-spin state, as an example, has a half-life almost 400-fold longer than expected from theory. On examining this relationship for alpha emitters of lower elements, it was found that as the energy of the second even-spin state increased, the hindrance factor decreased. For the species examined so far, the logarithm of the hindrance factor varies linearly with the atomic number (Fig. 2). There is no quantitative explanation yet known for the close agreement of this function. (It will be noted that a few points lie off the curve.)

If we assume that the same spin change is involved in each of these transitions, an explanation cannot lie in simple fashion in this direction both because of the large hindrance factors in some cases and because of the wide variation. A possible explanation lies in the assumption of a progressive change in charge asymmetry on leaving the closed shells in the vicinity of lead. The potential barrier will then be spherically nonsymmetrical and if the alpha particles of a type have a preferred direction of emission, any progressive change in charge distribution will be reflected in a progressive change in the ease with which the alpha particle can leave.

- ¹F. Asaro and I. Perlman, Phys. Rev. **87**, 393 (1952).
- ²S. Rosenblum and M. Valadares, Compt. rend. **235**, 711 (1952).
- ³A. Bohr and B. Mottelson, Phys. Rev. **89**, 316 (1953).
- ⁴Asaro, Thompson, and Perlman, Phys. Rev. (to be published).

High Altitude Measurements of the Intensity of Cosmic Radiation at Magnetic Latitudes 3°N and 19°N

A. S. RAO, V. K. BALASUBRAHMANYAN, G. S. GOKHALE, and A. W. PEREIRA
Tata Institute of Fundamental Research, Bombay, India
(Received June 8, 1953)

THE total intensity and penetrating component of cosmic radiation in the vertical direction have been measured as a function of altitude at Bangalore, magnetic latitude 3°N , and Delhi, magnetic latitude 19°N , during the years 1951–1953. Quadruple coincidence G.M. counter telescopes without any absorber and with 10 cm of lead absorber in between the counter trays were sent up in free balloon ascents to measure the total intensity and that of the penetrating component, respectively. The geometry of the telescopes was so designed that the most inclined particle recorded by the telescopes would only traverse a thickness of the atmosphere and the absorber 10 percent greater than a particle arriving vertically. The half-angles of the telescopes about the vertical were 13.5° and 24.5° . The temperature inside the gondola which contained the apparatus was maintained between $+15^{\circ}\text{C}$ and $+25^{\circ}\text{C}$ by using the greenhouse effect. The atmospheric pressure and temperature inside the gondola were measured by an aneroid and bi-metallic strip meteorograph of the Olland type. A mercury manometer was also used as an independent check on the pressure measurements. The atmospheric pressure, temperature inside the gondola, and the cosmic-ray data, were transmitted to the ground receiving station where they were recorded automatically on a moving paper tape.

The results obtained at the two stations Bangalore and Delhi are given in Fig. 1 as intensity vs pressure curves. Curves A¹ and B give the penetrating component at 3°N and 19°N , respectively, and C and D the total intensities at the above two latitudes. Every curve in the figure is a composite curve of the data obtained in a number of flights. The root-mean-square deviations of the points are marked for each curve.

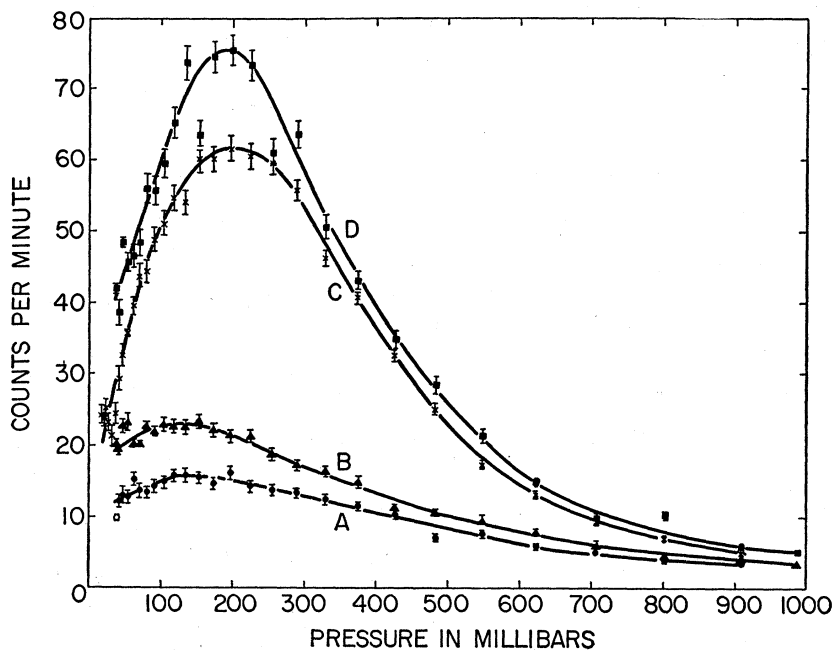


FIG. 1. Vertical intensity of cosmic radiation penetrating 10 cm of lead. A: at Bangalore 3°N (mag), B: at Delhi 19°N (mag). Total vertical intensity of cosmic radiation, C: at Bangalore 3°N (mag), D: at Delhi 19°N (mag).

The intensity of the component penetrating 10 cm of lead absorber at 3°N and 19°N increases continuously with decreasing pressure, reaches a maximum at a pressure of 120 millibars, and then falls with further decrease in pressure. However, the slopes of curves A and B on either side of the maxima differ from each other. The rise of curve B with decreasing pressure before the maximum is much faster than that of curve A, whereas the fall after the maximum is much less steep.

The total intensity at 3°N and 19°N (curves C and D) increases rapidly with decreasing pressure passes through a maximum at 200 millibars and then decreases very rapidly up to the lowest pressure obtained.

There is no detectable shift in position of the maxima between 3°N and 19°N, both in the case of the total intensity and the penetrating component. This may be due to the smallness in difference in the cut-off values of the primary radiation at the two latitudes.

Neher and Pickering² reported that there was no detectable increase in the total intensity of cosmic radiation at high altitudes in going from 3°N to 19°N, but our results are in disagreement with this and show that the ratio of the intensities is given by $I_t(19^\circ)/I_t(3^\circ) = 1.22$ at the maximum. For the penetrating component at the maximum, the corresponding ratio $I_p(19^\circ)/I_p(3^\circ)$ is 1.46. The latitude effects I_{19°/I_{3° for the total radiation and the penetrating component decrease with increasing pressure. The latitude effect at the maximum is much greater for the penetrating component than for the total cosmic radiation as the above figures show, whereas Vidale and Schein³ found that at 28°, 41°, and 55° the latitude effect for the total intensity was higher than that of the penetrating component.

The primary flux values obtained by extrapolation of the penetrating component curves, uncorrected for showers and accidentals, to the top of the atmosphere at 3°N and 19°N along 77°E geographic longitude are 227 and 364 particles meter⁻² sterad⁻¹ sec⁻¹, respectively. If the correction due to showers and accidentals, which is essential, is considered, the flux values may be smaller by 25 to 30 percent. The shower and accidental measurements have been made, but they are not used to correct the flux values as they do not extend below 75 millibars.

The theoretical analysis of these results, which is in progress, will be published soon.

We wish to express our gratitude to the Atomic Energy Commission, Government of India, for the grants which have made these experiments possible. We wish to express our thanks to Professor H. J. Bhabha for his great interest in the progress of the work and for helpful suggestions and criticism.

¹ Curve A, which has already been published [Phys. Rev. **83**, 173 (1951)], is given here for comparison with the results at 19°N (mag).

² H. V. Neher and W. H. Pickering, Phys. Rev. **61**, 407 (1942).

³ M. Vidale and M. Schein, Phys. Rev. **81**, 1065 (1951).

Measurements of Meson Masses and Related Quantities

F. M. SMITH, W. BIRNBAUM,* AND WALTER H. BARKAS
Radiation Laboratory, Department of Physics, University of California,
Berkeley, California

(Received June 12, 1953)

A MESON-MASS measurement program has been completed. The method has been partially described^{1,2} and preliminary results²⁻⁴ have been reported at earlier stages of the work. As noted previously,² it was discovered that stray mesons coming from points other than the target were interfering with the measurements. Attempts to reduce this effect have been successful, and little evidence of stray mesons remains.

To determine the pion masses, meson and proton ranges and momenta were measured in the same velocity interval. To measure the pion-to-muon mass ratio, similar comparisons were made between pions and muons. In one of the methods employed to find the momentum p_0 of the muon which is emitted when the pion decays at rest, the muon range is compared with the ranges of pions of known momentum and of nearly the same velocity. The decay muons were also compared directly with muons coming from the target in a second type of experiment.

For each particle, the quantity studied statistically is that function of the mass in which the range appears linearly. The dominant term in the variance of this quantity is the range straggling; consequently, it as well as other sources of variance has been examined closely, and the shapes of the measured distribution functions are now understood theoretically.

The stray mesons mentioned above introduced a systematic error of about one percent in the mass values quoted previously. The known systematic effects are now believed to be eliminated,